Reprinted from JOURNAL OF APPLIED METEOROLOGY, Vol. 31, No. 5, May 1992
American Meteorological Society

Automatic Tracking and Characterization of African Convective Systems on Meteosat Pictures

YVES ARNAUD

Laboratoire d'Hydrologie de l'ORSTOM, Montpellier, France

MICHEL DESBOIS

Laboratoire de Météorologie Dynamique du CNRS, Palaiseau, France

JOËL MAIZI

Informatique ORSTOM, Montpellier, France

(Manuscript received 6 February 1991, in final form 17 July 1991)

ABSTRACT

With the objective of building climatological statistics on propagating African convective systems and extracting pertinent parameters for the evaluation of precipitation an automatic method of tracking clouds with cold tops on Meteosat infrared (IR) images is established. This method takes into account eventual separation or merging of clouds. Results obtained in several cases not only demonstrate the capability of the method to perform correct tracking in different situations, but also show that objective determination of parameters, such as propagation speeds, system area, and volume index, is possible. The analysis of the time evolution of these last parameters allows a clear characterization of the cloud life cycle with its growing and decreasing stages, which may be useful for improving precipitation-estimation methods based only on cold-cloud occurrences or cloud-top temperatures.

1. Introduction

Numerous studies have been triggered by the research centered around explanations given for the Sahelian droughts that occurred during the years 1968–87 and that have been documented most notably by Nicholson (1981, 1985), Lamb (1985), and Sircoulon (1976, 1985). These studies concern both the investigation of large-scale mechanisms or teleconnections on an observational basis (Lamb et al. 1986; Greenhut 1981; Newell and Kidson 1984), as well as model sensitivity studies on the influence of changing conditions, such as surface albedo and sea surface temperature (Charney et al. 1977; Laval and Picon 1986; Palmer 1986). Both of these approaches require accurate descriptions of different climate parameters by conventional or satellite measurements. Over Africa the network of conventional measurements is rather poor, and the satellite data take on a certain importance, especially for the characterization of the convective systems that produce most of the rain over the region. Geostationary satellites (Meteosat for this area) allow the description of the life cycle of the events, as well as their motions and structure (Desbois et al. 1988; Duvel 1988). However, more systematic studies based on entirely objective data processing are still needed. These studies will allow improved diagnostic studies of the African climate and will also document the dynamics of the systems in relation to large-scale circulations, such as monsoon flow, low-level convergence of humidity, and tropical and African easterly jets. For synoptic scales and mesoscales, it will be possible to study the roles of diurnal cycle, orography, and easterly waves, for example, on statistical bases, but the methodology presented in this paper was originally developed for the purpose of the study of precipitations and precipitating systems over the Sahel.

Sahelian rains occur in a rainy season taking place from June to September, when the intertropical convergence zone (ITCZ) shifts to the northernmost latitudes during the annual cycle (around 20°N). These rains are produced by several kinds of cloud systems: large cloud clusters associated with monsoon rains in the southern part of the ITCZ cloud band and local convection and organized squall lines in the northern part. These last systems affect the Sahelian regions, where it is generally admitted that squall lines are the principal source of precipitation; although this depends on the definition of the squall line and on the orography of the area, as it was shown in Desbois et al. (1989).

Corresponding author address: Dr. Yves Arnaud, Laboratoire d'Hydrologie de l'ORSTOM, Centre de Montpellier, 2051 Avenue du Val de Montferrand, BP 5045 34032 Montpellier Cedex 1, France.

It is worthwhile to interpret the satellite cloud observations in terms of precipitation in those countries where the problem of rain is so crucial economically and where the measurements of the raingages are often not well distributed and sometimes unreliable. Numerous satellite rain algorithms have existed in the literature for a long time (see, for example, the review of Barret and Martin 1981), and research in this domain has recently been renewed again by the use of passive microwave data of the Special Sensor Microwave/Imager (SSM/I) and the future possibilities of satellites such as the Tropical Rainfall Measuring Mission (TRMM) (Theon and Fugono 1988). Because microwave methods are still being tested and the time sampling of these measurements will be poor due to the use of low-orbit satellites, the use of IR images from geostationary satellites is still necessary. In this domain, the simpler algorithms are generally based on principles close to the one of Arkin (1979), counting the number of occurrences (in space and/or time) of pixels corresponding to IR radiative temperatures below a given threshold. In Africa these kinds of techniques have been adapted, in operational routines, like the method of the TAMSAT group of the University of Reading (Dugdale et al. 1990) or that of the Office de Recherche Scientifique et Technique d'Outre Mer (ORSTOM) Lannion in France (Carn et al. 1989). However, many problems remain in the interpretation of such results; for example, validation of the algorithms by proper in situ measurements (see, for example, Arnaud and Thauvin 1990), stability of the relationships in space and time (Carn et al. 1989), precision of the estimations related to time and space scales (Jobard and Desbois 1989, 1992), and the effects of orography, surface properties, and the kind of tropical system. In order to understand these problems, it is necessary to investigate the relationships between cloud properties and rain at the scale of the events. It is well known from previous studies carried out, for example, in the United States that the relationships found are not stable from one event to the other; this has again been shown by Thiao et al. (1990) for Sahelian regions of Africa. However, these local-scale studies demonstrate the usefulness of a characterization of individual events and their phase of development for improving the precipitation evaluation.

The EPSAT (Estimation des Précipitations par Satellite)–Niger network (Hoepffner et al. 1989; Thauvin and Lebel 1989), involving 90 recording raingages (in 1990) and a weather radar on a test area of 100×100 km^2, has been devised in order to investigate the satellite in situ precipitation-estimation relationships at a time and space scale adapted to the African rain systems. The dense validation network allows us to receive more proper areal precipitation measurements, which somewhat improves the correlations with satellite indicators (Arnaud et al. 1990), but the variability of the relationship remains a problem, depending on the event and its stage of evolution when passing over the validation area. The purpose of this present paper is, thus, to present automatic methods that will enable objective characterization of the life cycle of the convective systems. After a presentation of the data and an analysis of the problem, we focus on the tracking of the systems; then the results of tracking and characterization are presented for different cases; finally, we discuss the usefulness and perspectives of our method for climate and precipitation remote-sensing studies.

2. Analysis of the problem, data, and general approach

Tracking and characterization of propagating African cloud systems has already been performed for research and even operational purposes. One of the first satellite studies was undertaken for the period of the GARP Atlantic Tropical Experiment (GATE) by Aspliden et al. (1976) using GOES data. Meteosat satellites, with their position above 0° longitude, have allowed a better observation of these systems since 1978, and manual tracking was performed in Africa as early as 1982 (Ago Ago 1982). Most of the studies of this kind restrict themselves to very simple extractions, such as the position of the front of the squall lines. More elaborate parameters resulting from the analysis of full-resolution digital images could not be produced on a significant number of cases due to the awkwardness in handling these kinds of data. An alternative was found in the use of sampled data produced for the International Satellite Cloud Climatology Program (ISCCP). Meteosat B2 data are sampled temporally every 3 h and spatially one pixel out of six in lines and columns, resulting in a 30-km resolution at the subsatellite point. These data were used for the tracking and characterization of squall lines in Desbois et al. (1988), mainly through interactive work on an image-processing system. In order to present valid statistics, the results were further extended by Gnamien (1990) to a larger number of months of three West African rainy seasons. However, this kind of work, requiring a lot of operator time, cannot be extended to systematic studies; it also introduces a part of subjectivity in the definition and tracking of events that can exhibit large changes at 3 h intervals (deformations, but also splitting or aggregating with other clouds). Due to these large deformations, it appears in the same paper of Desbois et al. (1988) that automatic tracking derived from the usual cloud-track wind techniques is not able to perform correct tracking of the squall lines at the scale of the ISCCP B2 data.

Taking this into account, and considering the specific necessity of a good spatial and temporal resolution for the applications concerning the study of precipitations at the scale of the cloud system, the present study uses full time and space resolution *Meteosat-4* data (30 min and 5×5 km^2) for cases of the 1989 rainy season. These images cover West Africa from Lake Chad to

the Atlantic (Fig. 4). The thermal infrared channel (10.5–12.5 μm) is used, and the cloudy pixels considered are only those that exhibit apparent radiative temperatures below −40°C, which is a commonly used threshold for separating convective rainy systems from other clouds.

Based on the observation of thresholded image sequences, the general principles of an automatic tracking algorithm have been defined:

1) Each image of the sequence to be processed is analyzed in order to label every cloud and to compute some characteristic parameters for each labeled cloud.
2) For a chosen cloud on a given image, the corresponding element(s) is (are) defined on the following image and is iteratively up to the dissipation of the system. New images are then created, keeping only the relevant cloud(s). The parameters of the system on each image are kept in a file.
3) Finally, this file is analyzed to produce parameters characterizing the life cycle of the event.

The results are partly conditioned by the definition of the formation and dissipation of the cloud system. In the present test study, the image sequence to be analyzed is chosen from the fact that at least one interesting propagating event has been observed over the EPSAT–Niger network. In the same way, the first cloud of a sequence is chosen interactively; which is not always that easy, since squall lines can originate either from local, isolated convection or from large convective areas such as south Chad/north Cameroon. The formation place of an interesting event can also be outside of our study area, that is, east of Lake Chad. The last image of the tracking is either a true dissipation (no more related cloud on the following image) or the merging of the system with more or less permanent cloud masses like those existing above Guinea or south Senegal. Detailed features of the processing sequence are given in section 3.

3. Method description

The infrared images are first calibrated according to the *Meteosat-4* calibration report (1989) and navigated following the procedure of the Meteosat system guide (1989). Afterward, the following treatments are applied on each image.

a. Thresholding

A threshold corresponding to a brightness temperature of −40°C is applied, similar to the ones often used for the separation of precipitating parts of tropical convective clouds. The pixel values that are colder than the threshold are kept, while the others are set to zero.

b. Clustering and labeling

Each connected ensemble of pixels with values different from zero (named cloud in the following) is then identified, and a common index (number of the cloud) is given to all the pixels of the same cloud (numeration). Clouds are numbered following the image scanning order. Due to the image encoding on 8 bits, the maximum number of clouds that can be counted in this way is 255. The resulting images represent each cloud with a particular value (number or index of the cloud). The labeling technique used is similar to the one used by Kermel (1987).

c. Parameters processing

For each cloud the following parameters are defined:

- area (in number of pixels);
- coordinates of the center of gravity, taking into account a weighting by the temperature of each pixel inside the cloud;
- maximum width (north–south) and length (east–west);
- position of the front edge, chosen as the westernmost x coordinate corresponding to the y coordinate of the center of gravity;
- moments of inertia, taking into account a weighting by the temperature of each pixel inside the cloud; and
- angle between the principal axis of the cloud and the x axis.

These results, obtained for each cloud, are stored in a file corresponding to the analyzed image.

d. Cloud tracking

The previous stages of processing provide an image sequence with indexed clouds and a parameters file sequence. The original images with radiometric values are also available. The purpose of the following steps is to follow a cloud, or rather a cloud ensemble associated to a perturbation, from birth to dissipation:

(i) The basic principle of the method is to consider the intersection between the clouds appearing on two successive images. The cloud $M(t + 1)$ on the image taken at time $t + 1$ is considered to correspond to the evolution of the cloud $N(t)$ on the image taken at time t when the intersection between $N(t)$ and $M(t + 1)$ is the greatest of all intersections of $N(t)$ with the clouds of the image taken at $t + 1$. A cloud selected interactively on an initial image can then be tracked step by step in the following scenes, as long as an intersection surface exists. The tracking end occurs either when there is no longer an intersection with a cloud of the following image (due to cloud dissipation or large propagation speeds of small clouds) or when the cloud merges with a very large cloud system of the ITCZ.

One drawback of this simple cloud tracking is that a cloud does not generally stay as a single connected entity during its life (it can split into two or more clouds, or include other ones). It is, therefore, insuf-

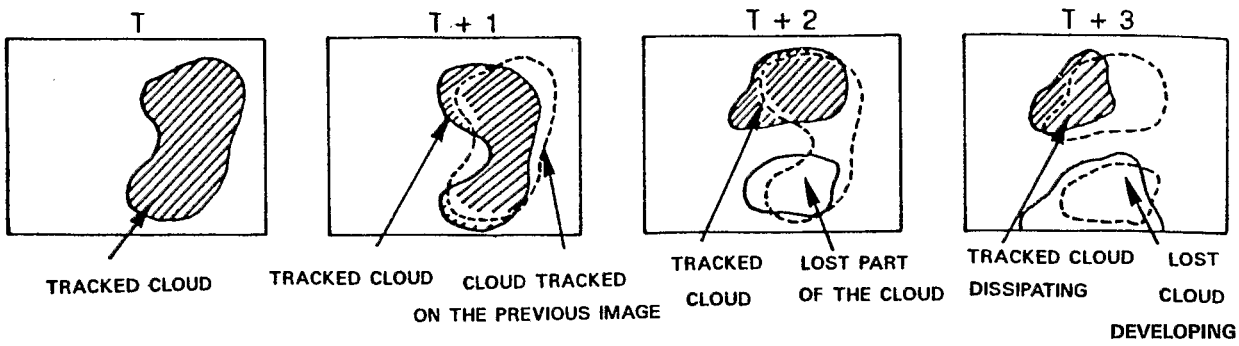

FIG. 1. Single-cloud tracking.

ficient to track only the cloud presenting the greatest intersection surface. For example, the cloud tracked originally can disappear while clouds originating from the same system persist for a longer time. It appears from the image sequences that it would be more consistent to track a perturbation composed of several clouds colder than the threshold rather than single clouds. Figure 1 illustrates the single-cloud tracking and gives an example of its problems.

(ii) A second scheme is proposed in order to overcome this problem. The cloud $M(t+1)$, corresponding to the evolution of the cloud $N(t)$, is now considered as the union of all the clouds $M_1(t+1) \ldots M_n(t+1)$ presenting an intersection with the cloud $N(t)$. All the clouds $M_1(t+1) \ldots M_n(t+1)$ will be considered in order to search for the following ones on image at $t+2$, and so on.

This method has also a straightforward drawback: in some cases, a chain reaction occurs, and other phenomena than the system we want to track are included. This occurs, for example, when a secondary cloud of the initial system meets another perturbation. Figure 2 illustrates such tracking and the associated drawback.

(iii) These considerations outline the necessity to limit the number of clouds tracked. This is done in the following way: the clouds $M_i(t+1)$ are arranged in decreasing order of intersecting surfaces. In order to be included in the ensemble of tracked clouds, the clouds $M_2(t+1) \ldots M_n(t+1)$ must fulfill the condition on the surface ratios:

$$\frac{[M_i(t+1) \text{ inter} N(t)]}{M_i(t+1)} > 0.5.$$

Thus, an extended cloud presenting a few common pixels with a secondary cloud of the previous image is discarded. It is worth noting that this condition is not applied to the main cloud, presenting the largest in-

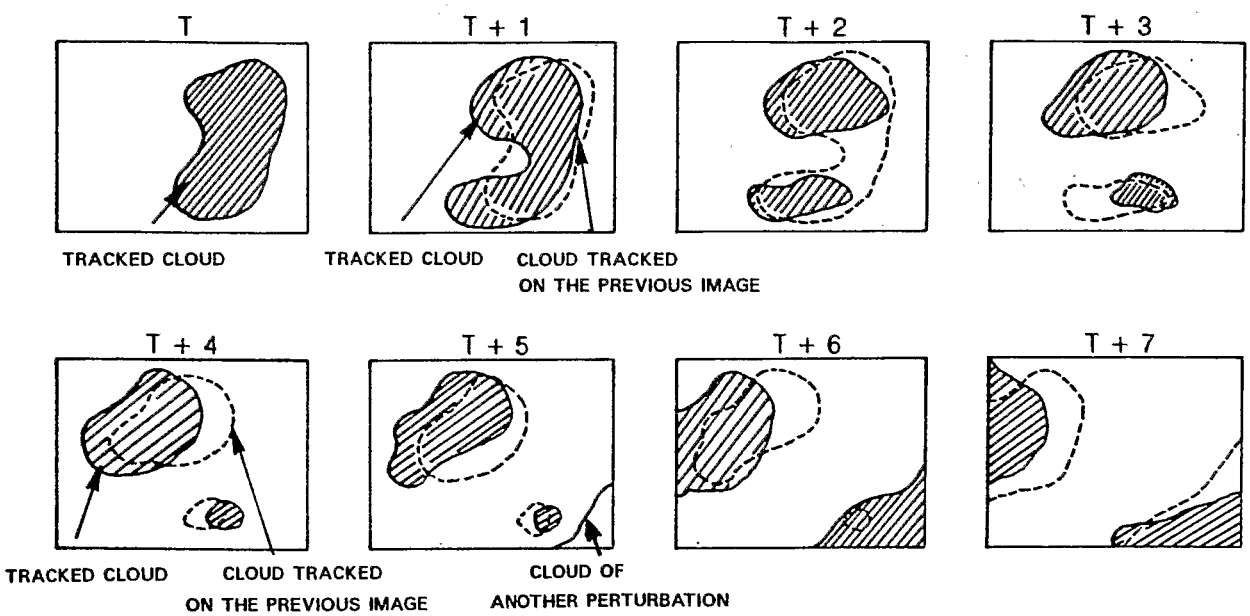

FIG. 2. Tracking all clouds presenting an intersection with the initial one.

tersection, $N_1(t+1)$, which is systematically kept. The choice of the value 0.5 for the surface ratio appeared to allow a correct tracking in the cases studied here, but other choices can be made according to specific situations. Figure 3 illustrates the tracking under these new conditions.

There are still some cases where this last method may cause some tracking problems, due to particular secondary clouds: secondary clouds ahead of the principal cloud have to be included, even if they do not fulfill the surface ratio conditions (they correspond generally to new cells developing ahead of the squall line); others may stray away from the perturbation and have an independent life cycle without merging with any bigger cloud. In general, however, they have short life times.

Another source of error is due to missing images in the time series: the aforementioned conditions have then to be adapted to the gap between the images, which induces smaller cloud intersections.

e. Processing of the parameters for the clouds selected in the event

The parameters obtained previously for the individual clouds, and some new ones, are then processed. These parameters are now related not to single clouds, but to cloud ensembles defined in section 3d. This leads to the definition of the new parameters:

- longitude and latitude of the center of inertia of the cloud ensemble,
- volume index (Szejwach and Desbois 1978) taking into account the number of pixels in each temperature range below the threshold.

The index volume is defined by $\sum n_i(T_i - T_0)$, where n_i is the number of pixels in the class i, T_i is the temperature of each pixel in the class i, and T_0 is the threshold temperature.

f. Determination of the event characteristics

Based on the temporal evolution of the aforementioned parameters, some characteristics of the life cycle of the studied event can be deduced; for example,

- latitude and longitude of first appearance
- latitude and longitude of dissipation
- duration
- trajectory length
- mean longitudinal speed of the center of gravity (average of the "instantaneous speeds" computed at the half-hourly step)
- mean longitudinal speed of the front edge

However, other parameters may be added to this list for particular purposes.

4. Results

The results presenting some selected events are discussed here. These events have been taken among the 25 events that produced more than 1 mm on at least five stations during the 1989 rainy season inside the validation network of EPSAT near Niamey (Fig. 4). The first step in assessing the quality of the results is by visualization of the images restricted to the isolated clouds. The comparison of the animations built from the image containing all the clouds and from the images of isolated systems, which represent the results of the algorithm exactly, allows us to qualify the tracking relative to what would have been found by human interpretation. Another way is the examination of the temporal evolution of the cloud parameters or of the relation between the parameters. Continuous evolutions indicate consistent tracking. This allows, for example, an evaluation of the improvement of the tracking between the single-cloud method and the final version of the method (Fig. 5). A significant improvement of the smoothness and continuity of the curve can be seen when applying the final method, indicating the tracking of a more consistent cloud ensemble. The remaining discontinuity (just before midnight on 18 August) is due to the merging of two perturbations.

Examples of time evolution of different parameters for some tracked events are shown below:

- Displacement of the center of gravity of the cloud system: Fig. 6 enables us to analyze the system trajectory for 4 August 1989. As for most of the systems of

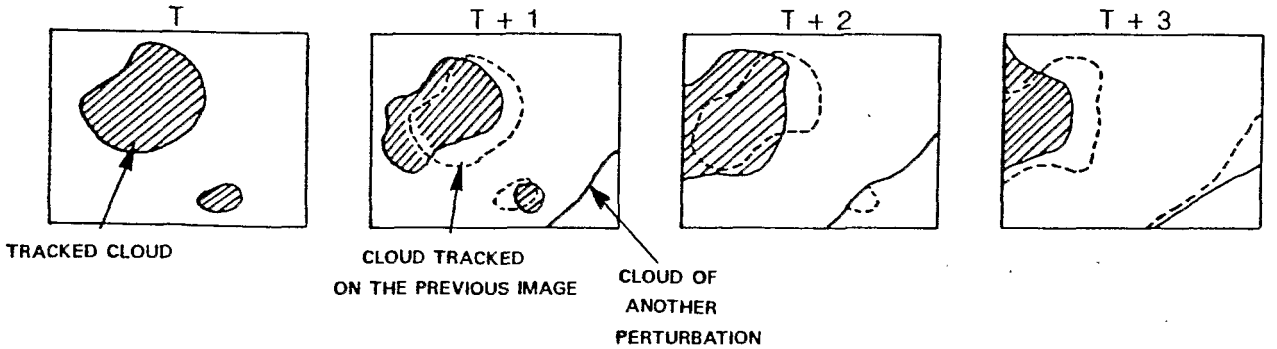

FIG. 3. Final cloud tracking.

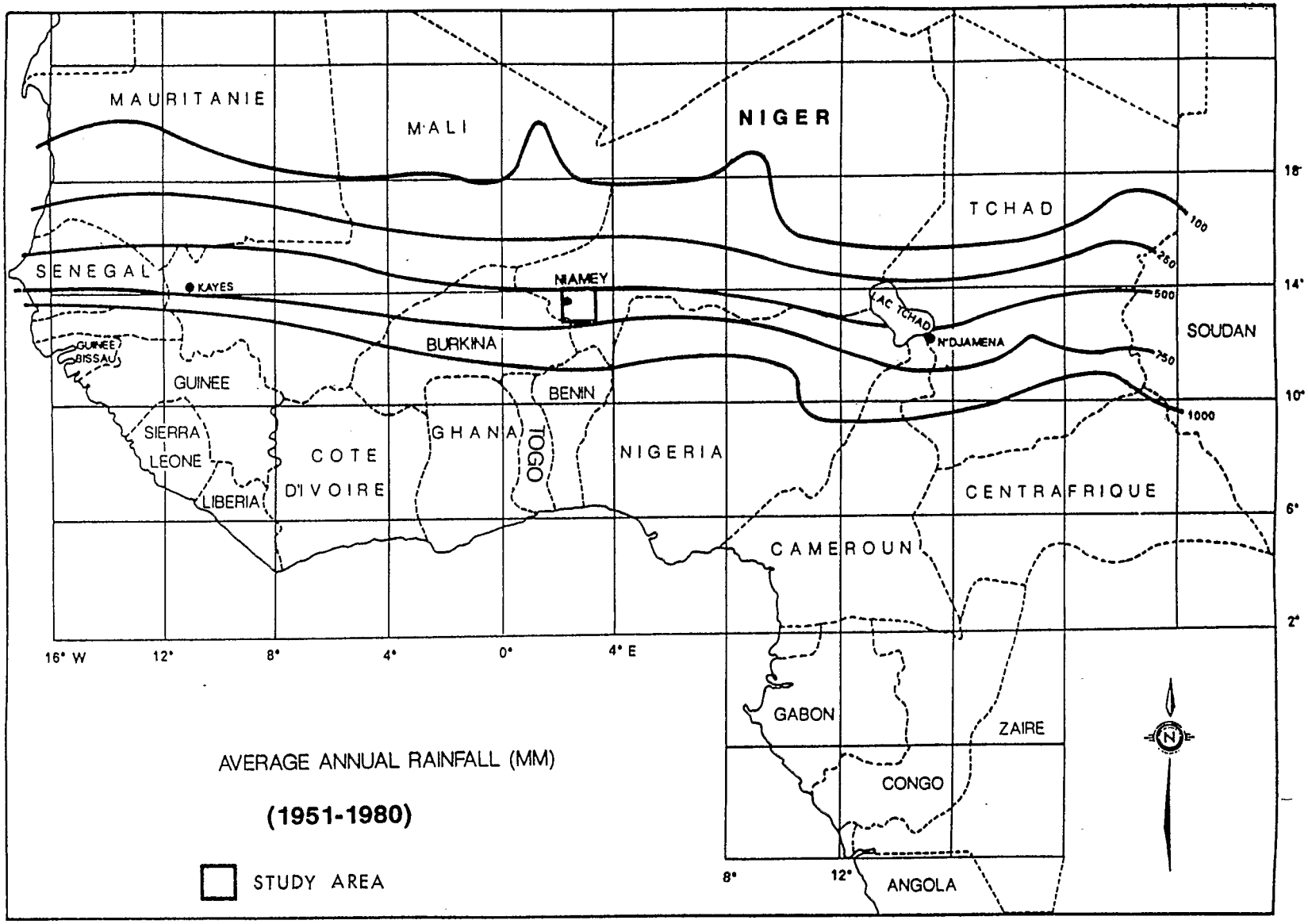

FIG. 4. Map of the study area (West Africa).

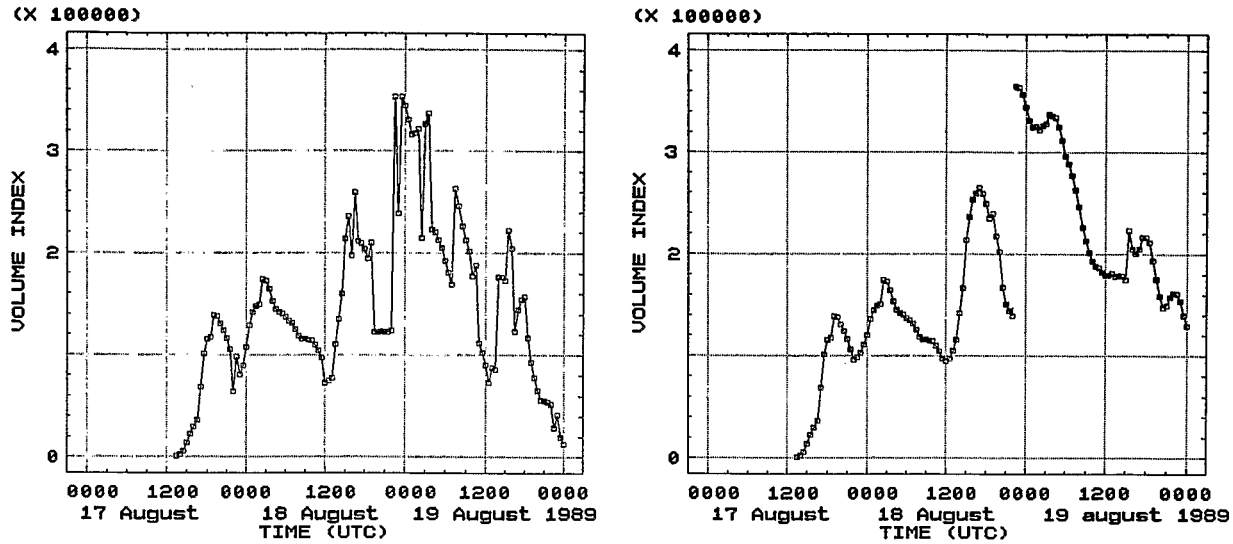

FIG. 5. Temporal evolution of the cloud volume index (% km^2 °C) (a) with the first hypothesis (b) and with the third hypothesis.

this region, this one propagates from the northeast toward the southwest. The discontinuity occurring at 12°N, 3°W is due to the merging of the system with a cloud previously located ahead of the perturbation.

- Temporal evolution of the cloud area: Fig. 7, for 18 August 1989, shows a continuous variation of this area, with the same discontinuity already mentioned for the volume index in Fig. 5. Elsewhere, the area is submitted to successive increases and decreases with time scales of several hours, corresponding to the modulations of the cloud activity by different factors, such as the diurnal cycle, the topography of the area, and large-scale or local meteorological conditions.
- Three-dimensional representation of the simultaneous evolution of the position of the center of gravity of the system and its cloud volume index is shown in Fig. 8 for 6 September 1989. This kind of representation is useful to easily relate the cloud development to geographical characteristics.
- Comparison of the displacements of front edge and center of gravity of the system. Figure 9, for 1 September 1989, shows a parallel displacement of these two points. However, the motion of the center of gravity is smoother than the one of the front edge, due to irregularities in the front shape of the clouds (new cells, accretions), which do not affect so much the position of the center of gravity.
- Relationship between the cloud volume index and the cloud area: for 11 July 1989 (Fig. 10), the plot of the volume index versus the surface appears to describe

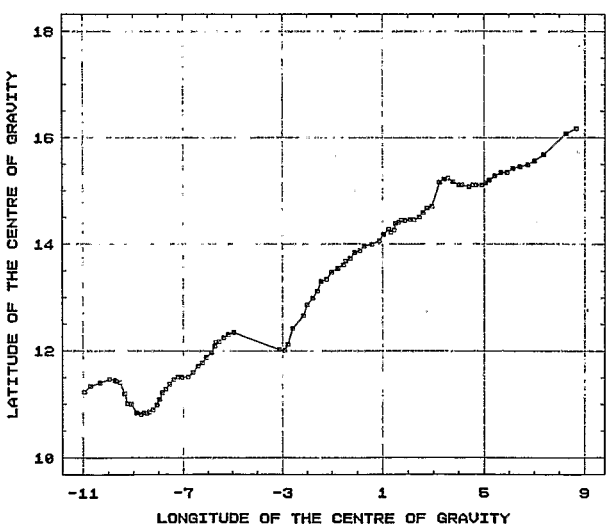

FIG. 6. Displacement of the center of gravity (degrees of latitude and longitude).

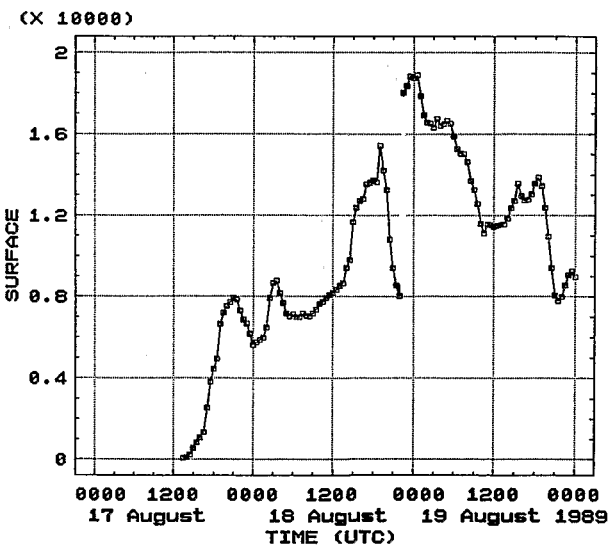

FIG. 7. Temporal evolution of the cloud area (in number of pixels).

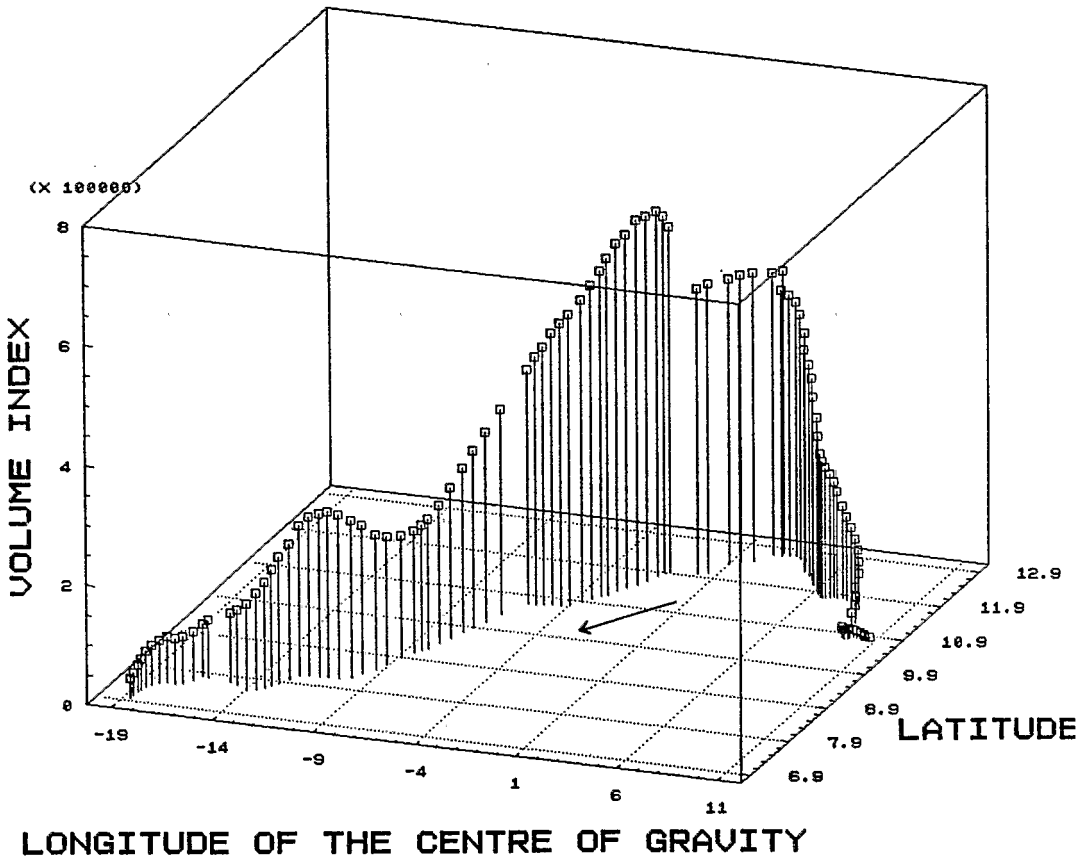

FIG. 8. Evolution of the cloud volume index (% km^2 °C) according to the location of the center of gravity (degrees of latitude and longitude).

a cycle with three successive phases, a growing of both surface and volume index (active convection), a growing surface and decreasing volume index (convection slowing down with decrease of the cloud-top height), and a decrease in both surface and volume index (dissipation stage). Note that the volume–surface ratio ap-

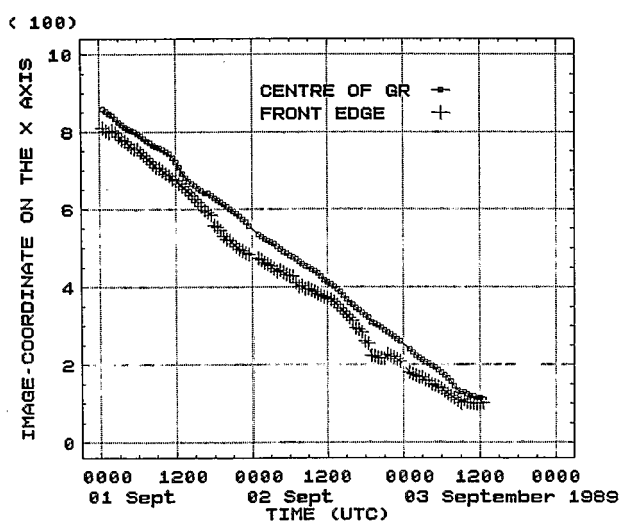

FIG. 9. Displacement (x image coordinate) of the front edge and of the center of gravity.

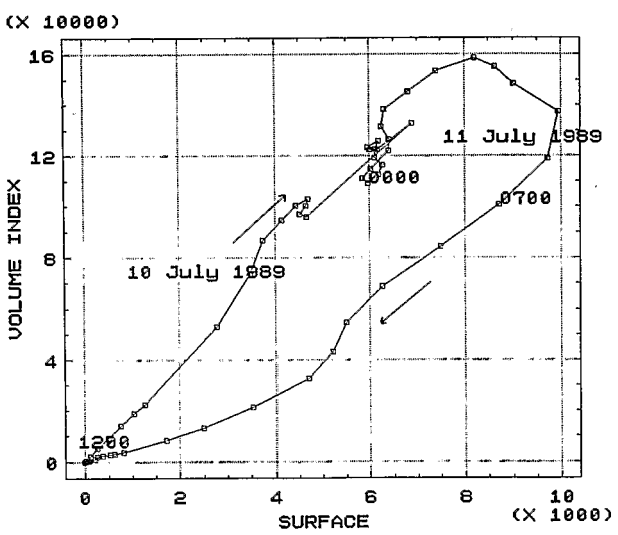

FIG. 10. Relation between the cloud volume index (% km^2 °C) and the cloud area (in number of pixels).

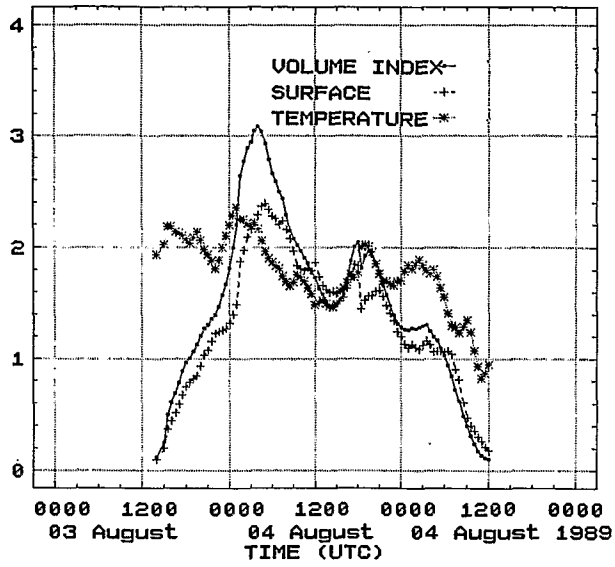

FIG. 11. Temporal evolution of the mean temperature (% °C), the volume index (% km^2 °C), and the surface (in number of pixels) of the cloud, respectively.

pears larger in the growing phase of the cloud than in the dissipating phase; this is a general characteristic that has been noticed for other events.

- Temporal evolution of the cloud mean temperature, volume index, and surface: another way to obtain indications on the dynamics of the clouds is the analysis of the temporal lag between these three variables. Figure 11, for 4 August 1989, shows that the decrease of temperature occurs first, then the increase in cloud volume index, and finally the increase in surface.
- General characteristics of some events in 1989: the cloud parameters defined make it possible to infer characteristics of the life cycle of the events. Table 1 shows examples of these characteristics, in a similar form as the results of Desbois et al. (1988), which were obtained from visual interactive processing of low-resolution images (Meteosat ISCCP B2). In the present case the automated algorithm enables processing of full-resolution images every half an hour, the main operator-dependent procedure being the choice of the initial cloud corresponding to one event (however, the choice of the time for first appearance is generally unambiguous). The definition of the final image of the sequence can be automatic, when the tracked event dissipates completely, or manual, when the tracked system merges with permanent clouds related to orography or ITCZ.

The times and places of first cloud appearance and dissipation, as well as the duration and length of the trajectory, depend to some extent on the operator choice, but the whole intermediate tracking is fully objective, reducing largely the analysis time. As the results presented here are restricted to a limited number of events, they do not allow us to build statistics on the climatic characteristics of squall lines. However, it can be noticed that the velocities found for the center of gravity of the systems (15.8 m s^{-1}) and for their front edge (17.2 m s^{-1}) are consistent with the velocities usually found from manual tracking. The difference between the two values is mostly related to the difference in the relative positions of the center of gravity and the front edge on the beginning and ending images of the tracking sequence (see, for example, the case of 1–3 September in Fig. 8).

5. Discussion and conclusions

The methods presented in section 4 are appropriate for the tracking of single clouds such as those related to diurnal convection, but can also deal with more complicated systems related to moving disturbances. These methods, based on simple principles of cloud labeling and intersections between successive images, are a little time consuming, especially related to cloud-tracking methods by correlation used for cloud–wind analyses. Moreover, they allow the simultaneous measurement of several cloud parameters that can be helpful for the definition of the cloud life history. Despite

TABLE 1. General characteristics for some events in 1989.

Event (1989)	Time of appearance (LST)	Time of dissipation (LST)	Place of appearance		Place of dissipation		Duration (h)	Trajectory length (km)	Medium longitudinal speed of the center of gravity (m s^{-1})	Medium longitudinal speed of the front edge (m s^{-1})
			Latitude (°N)	Longitude (°E)	Latitude (°N)	Longitude (°W)				
29 June	0051	2335	13°41′	09°01′	09°17′	02°31′	23.5	1474	15.3	22.2
10–11 July	1204	1540	14°01′	12°34′	15°01′	01°08′	28.5	1624	15.7	15.7
31 July–2 August	1509	1038	11°38′	06°10′	18°31′	16°43′	45	2759	17	17.2
3–5 August	1419	1101	16°10′	08°40′	11°14′	10°56′	46	2401	14	14.1
7–9 August	1429	1852	15°22′	11°08′	09°16′	13°14′	54	2988	14.9	17.1
17–19 August	1429	2312	16°16′	18°46′	12°49′	08°19′	58.5	3168	14.9	16.8
19–20 August	0105	2323	06°47′	12°56′	10°25′	05°37′	47.5	2287	13.1	15.1
1–3 September	0113	1109	11°09′	14°59′	11°33′	16°37′	60	3745	17.2	16.3
6–8 September	0157	0531	10°52′	10°38′	06°57′	18°37′	53.5	3532	17.8	19.5

some steps that are not fully automatic for the definition of cloud formation and dissipation, one can expect some advantages in using these methods in different fields of climatology, meteorology, and hydrology.

In climatology the method can be very useful in determining the principal areas of squall-line formation and dissipation, the mean velocities and directions of propagation, the life time of the systems, their extent and height, etc. These different elements can allow better discrimination among the different classes of systems, diurnal convection, squall lines, monsoon cloud clusters, and orographic clouds. Nevertheless, the number of events processed until now is not sufficient enough to establish statistical properties allowing discrimination of different classes of systems. The present limitations in this kind of application are twofold: 1) the necessity of further developments to determine automatically the sources and dissipations and to track systematically all the cloud events of an image sequence; 2) the heaviness of handling a large number of full-resolution images taken every half hour. The technical solutions to these problems exist but would still be cumbersome to implement. For example, preliminary time and space sampling of the images could be performed to alleviate the data processing, but the effect on the quality of the results has to be assessed. It can be said that accounting for the size of the events and their propagation speeds, the space sampling of ISCCP type would be less damaging than time sampling, because our method is based on the intersection of the clouds on successive images.

From the meteorological point of view, the time evolution of convection indices, such as the cloud volume index and the surface covered, constitute valuable information about the cloud dynamics. In particular, the behavior of the volume–surface ratio during the life cycle of clouds or cloud systems appears to be systematic, with a higher value during the growing phase than during the decrease of the cloud. It would be interesting in the future, for a more complete understanding of the cloud life cycle processes, to relate these cloud evolution indices to in situ meteorological data.

From the point of view of precipitation evaluation from satellites, it is well known that a cloud produces less rain in its decreasing stage than during its growth (Barrett and Martin 1981). Thus, the characterization of the phase should improve the rainfall estimation, particularly for short time scales. The phase can be characterized, for example, from the time evolution of the cloud surface during its life cycle, but it appears here that the volume-index–surface ratio could be used on a single image to characterize the phase. It has been verified on a larger dataset of events (25 events) that they all correspond to very similar values of the ratios, and that the discrimination of the phases is possible for about 80% of the cases. In a previous study (Arnaud and Thauvin 1990), a simple precipitation evaluation method, based on the minimum temperature reached by a pixel during the passage of a rainy event, was evaluated versus the ground truth of the raingage network of the square degree of Niamey, Niger. The results were encouraging, but the parameters of the linear relationship fluctuated depending on the event studied, as in other methods. The cloud-phase determination will be introduced in order to assess the eventual improvements it can bring to such estimations on a small space and time scale. Another application is the automatic selection of stations affected by a perturbation in order to analyze the rain productivity along the life of the clouds. Manually, this work requires significantly more operator time and it is not always objective, since it depends on the operator. In addition, the parameters extracted with the manual tracking are simpler than those obtained with the automatic tracking. Unfortunately, the raingage network in these countries (West Africa) is too sparse to provide a comprehensive depiction of the rainfall under the clouds. The network must be densified with other automatic transmitting data stations, which provide data in "near real time."

REFERENCES

Ago Ago, D., 1982: Etude des amas nuageux mobiles sur l'Afrique occidentale. *Mémoire d'Ingénieur des Travaux en Agrométéorologie,* CILSS PNUD OMM, 114 pp.

Annexes to the Meteosat 4 calibration report, 1989; Meteosat exploitation project. European Space Operation Centre, Darmstadt, Federal Republic of Germany.

Arkin, P. A., 1979: The relationship between fractional coverage of high cloud and rainfall accumulations during GATE over the *B* scale array. *Mon. Wea. Rev.,* **107,** 1382–1387.

Arnaud, Y, and V. Thauvin, 1990: Areal versus point rainfall for the calibration of TIR Meteosat data. A Sahelian application. *Proc. Int. Symp. Remote Sensing and Water Resources,* Enschede, International Association of Hydrogeologists (IAH) and the Netherlands Society for Remote Sensing, 75–84.

——, M. Desbois, and A. Gioda, 1990: Towards a rainfall estimation using Meteosat over Africa. *Proc. ASCE Int. Symp. Hydraulics/Hydrology of Arid Lands,* San Diego, CA, 311–316.

Aspliden, C. I., Y. Tourre, and J. B. Sabine, 1976: Some climatological aspects of West African disturbance lines during GATE. *Mon. Wea. Rev.,* **104,** 1029–1035.

Barret, E. C., and D. N. Martin, 1981: *The Use of Satellite Data in Rainfall Monitoring.* Academic Press, 340 pp.

Carn, M., J. P. Lahuec, D. Dagorne, and B. Guillot, 1989: Rainfall estimation using TIR Meteosat imagery over the Western Sahel (1986–1987). *Fourth Conf. on Satellite Meteorology and Oceanography,* San Diego, CA, Amer. Meteor. Soc., 126–129.

Charney, J., W. J. Quirck, S. H. Chow, and J. Kornfield, 1977: A comparative study of the effects of albedo change on drought in semiarid regions. *J. Atmos. Sci.,* **34,** 1366–1385.

Desbois, M., T. Kayiranga, and B. Gnamien, 1989: Diurnal cycle of convective cloudiness over tropical Africa observed from Meteosat: Geographic characterization and interannual variations. *Ann. Geophys.,* **7,** 395–404.

——, T. Kayiranga, B. Gnamien, S. Guessous, and L. Picon, 1988: Characterization of some elements of the Sahelian climate and their interannual variations of July 1983, 1984, and 1985 from the analysis of METEOSAT ISCCP data. *J. Climate,* **1,** 868–904.

Dugdale, G., V. D. McDougall, and J. R. Milford, 1990: Potential and limitations of rainfall estimates for Africa derived from cold cloud statistics. *Eighth Meteosat Scientific Users' Meeting,* Norköpping, Sweden, Eumestat, EUM PO8, 211–220.

Duvel, J.-Ph., 1988: Analysis of diurnal, interdiurnal, and interannual variations during Northern Hemisphere summers using METEOSAT infrared channels. *J. Climate,* **1,** 471–484.

Gnamien, B., 1990: Etude des lignes de grain Africaines par imagerie satellitaire. Thèse de Docteur de l'Université de Paris VII, 165 pp.

Greenhut, G. K., 1981: Comparison of temperature gradient model predictions with recent rainfall trends in the Sahel. *Mon. Wea. Rev.,* **109,** 137–147.

Hoepffner, M., T. Lebel, and H. Sauvageot, 1989: EPSAT Niger: A pilot experiment for rainfall estimation over West Africa. *Proc. WMO/IAHS/ETH Workshop on Precipitation Measurement,* St. Moritz, Switzerland, WMO/IAHS/ETH 251–258.

Jobard, I., and M. Desbois, 1989: IR satellite estimations of rains in Sahelian Africa: Study of different spatial and temporal resolutions. *Fourth Conf. on Satellite Meteorology and Oceanography,* San Diego, CA, Amer. Meteor. Soc., 61–62.

——, and ——, 1992: Remote sensing of rainfall over the tropical Africa using Meteosat IR imagery: Sensitivity to time and space averaging. *Int. J. Remote Sens.* (in press).

Kermel, F., 1987: Estimation du rayonnement solaire au sol à partir de données météorologiques ou d'images satellitaires. Thèse de Docteur de l'Université de Paris VI, 160 pp.

Lamb, P. J., 1985: Rainfall in sub-Saharan West Africa during 1941–1983. *Z. Gletscherkd. Glazialgeol.,* **21,** 131–139.

——, R. A. Peppfer, and S. Hastenrath, 1986: Interannual variability in the tropical Atlantic. *Nature,* **322,** 238–239.

Laval, K., and L. Picon, 1986: Effect of the change of the surface albedo of the Sahel on climate. *J. Atmos. Sci.,* **43,** 2418–2429.

Meteosat-4 Calibration Report, 1989a: Meteosat exploitation project. Issue 2. European Space Operation Centre, Darmstadt, Federal Republic of Germany, 13 pp.

——, 1989b: Meteosat exploitation project. Issue 3. European Space Operation Centre, Darmstadt, Federal Republic of Germany, 19 pp.

Meteosat System Guide, 1989: Magnetic Tape and Files Description. Meteosat exploitation project, European Space Operation Centre, Darmstadt, Federal Republic of Germany.

Newell, R. E., and J. W. Kidson, 1984: African mean wind changes between Sahelian wet and dry periods. *J. Climatol.,* **4,** 27–33.

Nicholson, S. E., 1981: Rainfall and atmospheric circulation during drought periods and wetter years in West Africa. *Mon. Wea. Rev.,* **109,** 2191–2208.

——, 1985: Sub-Saharan rainfall 1981–84. *J. Climate Appl. Meteor.,* **24,** 1388–1391.

Palmer, T. N., 1986: Influence of the Atlantic, Pacific and Indian oceans on Sahel rainfall. *Nature,* **322,** 251–253.

Sircoulon, J., 1976: Les données hydropluviométriques de la sécheresse en Afrique intertropicale. Comparaison avec les secheresses "1973 et 1940". In cah. ORSTOM ser. Hydrol., Numéro Special Sécheresse, **XIII,** 75–174.

——, 1985: La sécheresse en Afrique de l'Ouest. Comparaison des années 1982–1984 avec les années 1972–1973. In Cah. ORSTOM, ser. Hydrol., **XII,** 75–86.

Szejwach, G., and M. Desbois, 1978: Dynamic classification of mesoscale cloud patterns. *J. Appl. Meteor.,* **17,** 1406–1411.

Thauvin, V., and T. Lebel, 1989: Study of rainfall over the Sahel at small time steps using a dense network of recording raingauges. *Proc. WMO/IAHS/ETH Workshop on Precipitation Measurement,* St. Moritz, Switzerland, WMO/IAHS/ETH 259–266.

Theon, J. S., and N. Fugono, 1988: *Tropical Rainfall Measurements.* Deepack, 528 pp.

Thiao, W., D. L. Cadet, and M. Desbois, 1990: Estimation of rainfall due to squall lines over West Africa using Meteosat imagery. *Meteorol. Atmos. Phys.,* **42,** 69–76.